HHS Public Access

Author manuscript

J Control Release. Author manuscript; available in PMC 2020 January 10.

Published in final edited form as:

J Control Release. 2019 January 10; 293: 144–154. doi:10.1016/j.jconrel.2018.11.028.

Ultrasound-responsive droplets for therapy: a review

H. Lea-Banks[1,2], **M.A. O'Reilly**[1,2], and **K. Hynynen**[1,2,3]

[1]Physical Sciences Platform, Sunnybrook Research Institute, Toronto

[2]Medical Biophysics, University of Toronto, Toronto

[3]Institute of Biomaterials and Biomedical Engineering, University of Toronto, Toronto

Abstract

The last two decades have seen the development of acoustically activated droplets, also known as phase-change emulsions, from a diagnostic tool to a therapeutic agent. Through bubble effects and triggered drug release, these superheated agents have found potential applications from oncology to neuromodulation. The aim of this review is to summarise the key developments in therapeutic droplet design and use, to discuss the current challenges slowing clinical translation, and to highlight the new frontiers progressing towards clinical implementation. The literature is summarised by addressing the droplet design criteria and by carrying out a multiparametric study of a range of droplet formulations and their associated vaporisation thresholds.

Keywords

Phase-change emulsions; focused ultrasound; cavitation

1. Introduction

Micrometre-sized gas-filled bubbles, known as microbubbles, were originally developed as ultrasonic imaging contrast agents. Using lipid, protein, polymer or surfactant shells, these gaseous vesicles have been designed for enhanced imaging and disease diagnosis, with slow dissolution in the blood, easy reconstitution for clinical use, and simple and safe implementation [1]. Microbubbles experience ultrasound as sequential changes in pressure, dynamically responding to each pressure perturbation by shrinking and expanding. When excited with sufficient amplitude, the bubble radius and incident pressure become non-linearly related, meaning the bubble may rebound upon collapse, exhibit prolonged expansion or implode entirely. Bubble activity of this kind is broadly termed acoustic cavitation and each behaviour is associated with a unique acoustic emission - producing

Corresponding author: Harriet Lea-Banks, Physical Sciences Platform, Sunnybrook Research Institute, 2075 Bayview Avenue, Toronto, ON M4N 3M5, Canada, harriet.lea-banks@sri.utoronto.ca.

Competing Interests

The authors have declared that no competing interests exist.

harmonic, ultraharmonic, subharmonic or broadband frequencies - each of which have been widely exploited for imaging and treatment monitoring [2].

Throughout the last decade the presence of acoustically excited microbubbles has been shown to increase the penetration depth of co - injected therapeutics into the surrounding tissue through a combination of dynamic phenomena: most notably, acoustic radiation forces [3] and microstreaming [4]. Furthermore, techniques for loading drugs into, onto and within microbubble formulations have been well developed and reviewed, allowing triggered and targeted release of therapeutics upon exposure to diagnostic levels of ultrasound [5]. However, the circulation time of microbubbles *in vivo* is notoriously short, influenced by physiological temperature and ambient pressure, where the dissolution of bubbles is driven by the diffusion of encapsulated gas into the surrounding blood. The longevity of microbubbles in circulation may be further compromised by drug-loading which has been reported to influence shell stability [5]. Furthermore, microbubbles respond to very low amplitudes of ultrasound, which is advantageous for imaging but in therapy may lead to off-target effects when bubbles are excited outside of the intended target region. Liquid emulsions in droplet form offer a stable alternative.

Oil emulsions, stabilised by surfactant coatings, have been widely utilised in the clinic, such as in aerosol therapies and the delivery of penicillin droplets stabilised with propylene glycol [6]. More recently nano-emulsions have found use in gene therapy and transdermal delivery [7]. However, to enable triggered release of a therapeutic payload, liquid cores with lower boiling points can be used, such as perfluorocarbons. This low-boiling point core is described as being superheated. The phenomenon of a superheated core is made possible by the surface tension provided by the shell, creating a pressure difference between the internal and external environments, known as the Laplace pressure. This pressurised core allows a compound, which in a free environment would be gas, to remain in a liquid state. The liquid-core droplet remains stable until exposed to an external stimulus, such as focused ultrasound, whereby an incident pressure perturbation induces a liquid-to-gas transition (figure 1), giving rise to the term ‘phase-change emulsion’. Figure 1 illustrates this process with an example nano-scale droplet that vaporises into a 1 μm-diameter bubble. The acoustic emissions detected from the construct increase in magnitude (shown in the voltage traces) and harmonic content (shown in the frequency spectra) upon vaporisation.

The mechanisms driving this vaporisation process have only recently been elucidated, and were previously reported to be triggered by internal cavitation nuclei [8], external cavitation nuclei [9], internal heating [10]. However, the most recent theory of acoustic droplet vaporisation, developed by Shpak *et al.* [11], describes the superharmonic focusing of acoustic energy inside the droplet which causes a spot of negative pressure that spreads throughout the liquid volume. The onset of vaporisation is shown to be instigated by the high-order harmonics produced through nonlinear propagation of the incident acoustic wave, and the subsequent focusing of the distorted waveform inside the droplet due to its spherical geometry and change in acoustic impedance.

When microbubbles are too fragile and non-specific, perfluorocarbon (PFC) droplets offer a stable solution for a cavitation agent with the therapeutic potential of microbubbles, drug-

loading capabilities and high specificity in localisation of triggered vaporisation and therapy. When compared to microbubbles, droplets have been shown to have a significantly longer circulation time *in vivo,* since the liquid core prevents gas dissolution. Due to their impressive stability and tuneable size, droplets have found use in a variety of potential diagnostic applications including fluorine-19 magnetic resonance imaging [13], positron emission tomography (PET) [14] and ultrasound imaging [15, 16]. Although a diverse range of imaging applications exist, the current review will focus on the use of ultrasound-responsive PFC droplets for therapy, both through bubble effects and as delivery vehicles for pharmaceuticals.

1.1 Bubble effects: therapy by cavitation

Focused ultrasound has the ability to achieve therapeutic results, from tissue ablation [38] to neuromodulation [39, 40] and neurogenesis [41]. However, the addition of cavitation agents and pharmaceuticals has now been shown in human clinical trials to enhance therapy through both thermal [42] and mechanical [43] mechanisms. Ultrasound can heat, produce bubbles, push drugs and cause fluid streaming [44]. With the addition of bubbles, heating can be enhanced, bubbles can dynamically respond and create scattered pressure fields, increase fluid mixing through microstreaming and open pores in cell membranes [45]. However, the stability of gas-core constructs is limited by dissolution of the gas into the blood and a characteristically low inertial cavitation threshold, leading to a construct with a short lifespan *in vivo.* By using a liquid-state PFC core, these limitations can be overcome.

The first set of applications for phase-change droplets exploit how ultrasound can transform them into microbubbles, and utilise these dynamically responding bubbles for tumour ablation [17], sonothrombolysis [18] or simply obstructing blood flow into tumour tissue[19]. In these applications, droplets may be triggered with more precise localisation than microbubbles because of their steep vaporisation threshold. Furthermore, when droplets undergo vaporisation they can expand to over 5 times their original diameter [19] (figure 1). During this expansion phase gas from the surrounding liquid is taken up by the construct, leading to novel applications such as oxygen scavenging [20, 21]. More recently, the ability of droplets to induce sonoporation has been studied [22]. Using a suspension of pancreatic cancer cells, the vaporisation of nearby droplets was shown to enhance the permeability of cell membranes, as illustrated by the uptake of an indicator molecule.

1.2 Pharmaceutical effects: cavitation-mediated drug delivery

The second set of therapeutic applications of droplets exploits their ability to encapsulate, carry and release a drug. With appropriate design, droplets have the ability to release a therapeutic payload upon sonication at a specific site. This localised, trigge red release may be further enhanced by the dynamic response of nearby vaporised droplets, which have the ability to propel therapeutics deeper into surrounding tissue, through secondary radiation forces and microstreaming. Stable cavitation can enhance drug delivery through better drug distribution [4], deeper penetration [46], permeabilization of nearby membranes [47] and localised release [48, 49], with the additional potential for real-time acoustic monitoring [50, 51] and localisation [52].

Of note are the oncological studies performed by Gao *et al.* [23] and Rapoport *et al.* [24], both using a copolymer shell (see section 4) to encapsulate doxorubicin (DOX) and Paclitaxel (PTX) respectively. As is well known, tumour vasculature is 'leaky' by nature, with endothelial pore size increasing from 20 nm in healthy vessels to 2 μm in certain solid tumour types [25]. Therefore nano-scale therapeutics, including droplets, have the ability to pass through pores in leaky vessel walls and enter the surrounding tissue, where they are retained due to the poor lymphatic drainage associated with cancerous tumours. Once embedded, droplets have the potential to vaporize in the cancerous tissue, allowing localised drug delivery from the accumulated constructs [26, 27].

In the growing field of oncolytic gene therapy, Gao *et al.* [28] have utilised PFC droplets for their diagnostic and therapeutic capabilities. The multi-functional construct was able to deliver gene therapy agents to HER2-expressing xenografts by co-loading liquid PFC and nucleic acids within a polymer shell decorated with targeting peptides. Through localised vaporisation of the droplets, the efficiency of gene transfection was significantly enhanced.

Furthermore, droplets offer the potential to treat small volumes and have less interaction in the near field compared to gas-core drug carriers [29]. This acoustic stability has been shown to allow a volume smaller than the ultrasound focal region to be treated, without compromising the ultrasound penetration depth, making droplets an attractive alternative to microbubbles as acoustic-responsive drug carriers.

2. Current challenges

Although the use of phase-change PFC droplets for therapy has gained significant interest over the last two decades, several key challenges have slowed clinical translation. The first of these is posed by the elementary decision of droplet components: which materials will form the encapsulating shell and the PFC core? Sheeran *et al.* [16] describe the optimal balance of thermal stability and vaporisation threshold - producing a construct that will remain unchanged at physiological temperatures, but with a low enough vaporisation threshold as to transition into a microbubble without causing tissue damage.

A further barrier to clinical translation is found in the discrepancies between *in vitro* and *in vivo* findings for vaporisation thresholds. It is widely known that ambient temperature plays a significant role in droplet behaviour, and efforts are made to conduct *in vitro* experiments at 37 °C [10, 15], however, a disconnect between phantom and animal studies still exists. Rojas *et al.* [30] have explored why greater acoustic pressures are required to instigate vaporisation *in vivo.* Their findings show that although hydrostatic pressure has no influence on the threshold, vessel diameter is influential, and decreasing the vessel diameter increases the pressure required for vaporisation; this finding was also observed by Lin *et al.* [31]. Furthermore, Wu *et al.* [32] have recently shown the importance of vaporisation *efficiency:* how many bubbles are produced upon sonication. Their findings show that, depending on the PFC core, the vaporisation efficiency can be very low *in vivo,* requiring greater sonication pressures to achieve the same treatment, increasing the apparent vaporisation threshold.

Thus far cancer therapy has been the avenue explored most extensively for therapeutic droplets. However, alongside substantial recent developments in clinical applications of trans-cranial focused ultrasound [33, 34] applications of droplets for drug delivery to the brain are coming to the fore [35, 32, 36]. When using droplets for drug delivery to the brain, exploitation of the vaporisation threshold for safe, efficient drug release is often sought without inducing inertial cavitation, since violent bubble collapse has been associated with damage of cerebral tissue [37]. This is a particularly challenging problem since the low frequencies associated with good penetration through the skull (due to reduced attenuation) increase the likelihood of inertial cavitation (due to extended rarefractional phase of each acoustic cycle) [37]. Separation between the vaporisation and inertial cavitation threshold has been shown to decrease at lower frequencies [10], requiring precise tuning of the sonication pressure to achieve drug delivery without causing tissue damage or haemorrhaging (section 8).

Recent developments in droplet design have sought to address these challenges and overcome the barriers to clinical translation. The current review will discuss a number of commonly used fabrication techniques, formulations and their appropriate applications, as summarised schematically in figure 2.

3. Fabrication method

A variety of techniques have been developed for the fabrication of phase-change PFC droplets, and may be categorised into the following; agitation, sonication, extrusion, condensation and microfluidic techniques (table 1). The methods range in complexity from simply shaking by hand [54, 55] to the manufacture of bespoke microfluidic devices using soft lithography [56]. In general, agitation methods are able to achieve micron-scale emulsions simply and rapidly. Furthermore, the entirety of the droplet solution is contained within a single vesicle, mitigating any material losses associated with microfluidic methods. However, agitation techniques often produce a wide size distribution and low reproducibility between batches.

In contrast, ultrasonic techniques are able to produce nano-scale droplets with a tighter size distribution, but may still require size exclusion processes such as filtration or the iterated use of a ‘microfluidizer’. Using a tip sonicator is a simple and popular approach, but can be compromised by cross contamination between samples and the introduction of metallic particulates into the emulsion as the tip erodes with use. Furthermore, both agitation and sonication techniques can cause the emulsion to heat up. Careful consideration of the temperature sensitivity of the droplet structure and the encapsulated therapeutic is required with this method. Microfluidic techniques offer a much tighter size distribution, created either through bespoke setups [57] or commercial systems such as a Microfluidizer Processor (M110-EHI, Microfluidics, Newton, MA, USA) [10]. Although the reproducibility and consistency of these techniques is much higher, the ease and speed of manufacture may be limited, especially in small microfluidic chip dev ices where droplets are produced individually [56, 57].

Additional protocol amendments are dependent on the choice of PFC and shell material. For low-boiling point PFCs it may be necessary to carry out fabrication on ice, dry ice or in a cold room, or by microbubble condensation (section 5). Furthermore, if polymer coatings are used it is common to begin by forming precursor micelles before introducing the PFC [58]. A range of these fabrication techniques are comprehensively reviewed by Sheeran *et al.* [16] for the application of ultrasonography.

4. Shell composition

In order for the superheated liquid core to be contained, a shell is required with sufficient surface tension such that the Laplace pressure is great enough for the pressurised centre to remain liquid at physiological temperatures, as described in section 1. Surfactants, proteins, lipids and polymers exhibit a variety of surface tension values (table 2 and figure 3) and are able to achieve liquid encapsulation to various levels of success depending on the desired application and droplet size.

Albumin has been used extensively to form PFC droplets for tumour ablation [17] and other therapeutic applications [55, 9, 59], including the formation of torodial bubbles [12]. Surfactants have also been explored due to their ability to appreciably lower surface tension, as seen in figure 3. In particular Zonyl FSO fuorosurfactant has been used in a number of studies, including the formation of 220 nm droplets for ultrasound imaging of *in vivo* tumours [15], and 100 − 600 nm droplets for sonothrombolysis [18]. However, both studies (which both implement DDFP cores) required considerable peak negative pressures to induce vaporisation - in excess of 5 MPa at 5MHz, with 1 ms bursts.

Commonly used to fabricate microbubble contrast agents, liposomes offer an elasticised shell. Elastic deformation of a lipid membrane allows for repeated expansion and collapse, optimal for therapeutic applications which exploit bubble effects. This elas tic behaviour exists until a critical expansion ratio is reached, as described by models such as the Marmottant model for the oscillation, rupture and buckling behaviour of large lipid-coated bubbles [60]. Behaviour such as lipid shedding [61] has also been reported, which may be beneficial for drug delivery [62]. Both single lipid formulations [63] and mixed lipid formulations [64, 10] have been successfully implemented in the fabrication of acoustically-responsive droplets.

The newest family of droplet shell compounds are PEG-based polymers, including diblock copolymer constructs [23, 24]. PEGylated nano-scale constructs are now widely used as drug delivery vehicles due to their stability and long circulation *in vivo,*resulting from the minimal protein absorption on the PEG-coated surface [65]. Furthermore, the ability to use diblock copolymers (with a hydrophobic and hydrophilic end, behaving like a synthetic lipid) facilitates the loading of lipophilic drugs with high loading efficiency resulting in therapeutically relevant dosages [35]. The fabrication of polymer droplets requires a unique formulation process: firstly a polymeric micelle is constructed with the lipophilic drug solubilised in the core (which alone may be used as a micelle drug-carrier) [66]; secondly the PFC compound is added. This two-stage process is comprehensively detailed by Rapoport [58].

It should be noted that surface tension is just one feature of the shell and many other characteristics play a part in determining the stability and response of a droplet, including nonlinear elasticity, shear modulus [68] and lipid inter-chain cohesion [69]. Lacour *et al.* [68] have explored this recently illustrating the strong influence of the nonlinear elasticity and stiffness of the shell on the vaporisation behaviour. The study concludes that the most favourable shells for droplet vaporisation are soft, with a low shear modulus and significant nonlinearity.

5. Core composition

Droplet cores are typically filled with superheated liquid-state perfluorocarbons (PFC), molecules formed from carbon and fluorine atoms configured in long chains. Compounds found within the PFC family differ in configuration and chain length, giving rise to unique molecular weights, densities and boiling points, as summarised in table 3. These unique features impart specific properties to the resultant droplets. Once the droplet has transitioned into a microbubble, the low solubility of the PFC compound slows the dissolution of the bubble into the surrounding fluid.

The vast majority of studies to date have selected dodecafluoropentane (DDFP) [55, 17, 9, 59, 10, 15, 18, 35]. However, alternative PFCs may offer important advantages. For example, perfluoro-15-crown-5-ether (PFCE) is a fluorine-19 MR imaging contrast agent which has been shown to have greater storage stability than DDFP [70, 13]. It should be noted that the potential toxicity of PFCE has been brought into question, with observations of extremely slow clearance in the liver and spleen [71]. Further investigation is required to elucidate the toxicology of PFCE.

A different approach was taken by Kawabata *et al.* [63] whereby a mixture of dodecafluoropentane (DDFP) and 2H,3H-perfluoropentane (DFP) was implemented and found to reduce the vaporisation threshold. It is hypothesised that the lower boiling point DDFP (29°C) which vaporized first, was able to act as a trigger to induce vaporisation in the higher boiling point DFP (55°C). Exploiting a similar mechanism, the use of quantum dots as cavitation seeds was applied first by Gorelikov *et al.* [8] and later by Martin *et al.* [72] in the application of fluorescence imaging of PFC droplets to study their interaction with cells. Here the droplets were loaded with silica-coated quantum dots which could be visualised *in vitro* and were found to lower the vaporisation threshold when compared to droplets not containing quantum dots. The same effect was observed by Lee *et al.* [73], where the inclusion of iron oxide nanoparticles for magnetic drug targeting lowered the vaporisation threshold of DDFP droplets.

For many applications the use of micron-scale droplets is not optimal. Since droplet radius is inversely proportional to vaporisation threshold [55], a nano-scale droplet requires a PFC with a lower boiling point to achieve a similar vaporisation threshold. Octafluoropropane (OFP) offers a very low boiling point and has therefore been used for applications requiring <200 nm sized droplets, such as sonoporation in oncology, where the droplet is intended to passively accumulate in the tumour tissue through the leaky vessels [22]. Using such low boiling point substances necessitates additional techniques and precautions during

fabrication [16]. Briefly, since pressure, temperature and volume are intrinsically linked, methods for condensing and containing a superheated liquid into a small vesicle naturally require sub-zero temperatures and an increased ambient pressure. These two elements can be applied in the formation of perfluorobutane (DFB) and OFP droplets through the condensation ofprecursor microbubbles. The use of highly volatile PFCs for ultrasound imaging has been reviewed in-depth by Matsunaga *et al.* [74].

6. Size and size distribution

The optimal droplet size depends on the intended therapeutic application (figure 2). Therapeutic applications exist both within the confines of the vessel - including endothelial targeting [75], sonothrombolysis [18], embolotherapy [53] and blood-brain barrier opening [76] - and beyond the vasculature, including the delivery of chemotherapeutic agents [26]. In embolotherapy, the blood supply to specific regions of tissue, such as tumours, is intentionally occluded. Droplets, tailored in size, may be used to achieve this, through expansion due to vaporisation and subsequent blocking of vessels. M. Zhang *et al.* [53] were able to show that, in the study of a canine kidney, both albumin- and lipid-coated PFC droplets are able to block pulmonary capillaries when at a size of 3 μm or greater (table 4). They comment also on the importance of a tight size distribution, sta ting that removing the ‘useless droplets’, those that were less than 1 μm and did not cause vessel occlusion, would enhance the desired effects. By the same merit, it is also important to identify the size of droplets which pass freely along blood vessels to achieve systemic delivery. Further still, many therapeutic applications require droplets to escape the vasculature entirely. Tailoring droplets to exploit the enhanced permeability and retention (EPR) effect in cancerous tissue may be advantageous for extravasation beyond the confines of the endothelial layer and accumulation of the construct at the target site [26].

The influence of droplet size on vaporisation threshold has been well documented both experimentally [55] and computationally [11, 77], where droplet diameter and vaporisation threshold are inversely proportional (figure 4a). Additionally, for drug-loaded droplets size also determines loading capacity. A characteristically high vaporisation threshold and low loading capacity form two key challenges for nano-scale droplets designed to exploit the EPR effect.

7. Concentration

The optimal droplet concentration is determined by safety and treatment efficacy. The safety of injecting gases into the body has been thoroughly investigated in the use of microbubble contrast agents, where, in the case of SonoVue, 16μL of sulphur hexafluorid e is the clinical dose. However, 10 times this volume has been found to be safe in humans [78]. In the case of droplets which exploit bubble effects for therapy, treatment efficacy is strongly influenced by the vaporisation threshold and efficiency [32]. The vaporisation threshold has been found to be influenced by droplet concentration, particularly when concentration values differ by orders of magnitude [79]. However, within relatively small changes in concentration, vaporisation threshold has been shown to be unchanged, as in the study by Zhang *et al.* [17], where no change was found in the droplet volume fraction range 0.15 − 0.40%.

For therapeutic droplets that are loaded with a drug, pharmaceutical dosage becomes an additional requirement. Therefore the droplet concentration must be sufficiently high as to deliver a therapeutically relevant dosage (with a low vaporisation threshold and thermal stability at 37°C) and sufficiently low for safe levels of gas injection. If the drug-loading efficiency is low, more droplets will be required to induce the same therapeutic effect. However, this carries a higher risk of bubble coalescence (which makes the co nstruct too large and shifts the resonance frequency) increasing the likelihood of embolism, damage from inertial cavitation, and acoustic shielding due to bubble clouds (which reduces the amount of ultrasound able to reach the entire droplet population). Ultimate ly the size, concentration and loading capabilities need to be optimised and tailored for the specific application, to ensure a safe and effective treatment strategy.

8. Vaporisation and inertial cavitation thresholds

The vaporisation threshold is defined as the magnitude of ultrasound pressure required to convert a liquid droplet into a gaseous microbubble. Once a droplet has become a microbubble it continues to respond to ultrasound, either by stably pulsating or, with sufficient ultrasound energy, by expanding significantly and becoming unstable, collapsing inwards from the inertia of the surrounding fluid. This unstable behaviour is known as inertial cavitation. Therefore the inertial cavitation threshold for a droplet may be defined as the magnitude of ultrasound pressure required to observe this unstable collapsing behaviour.

Throughout the literature, short pulses of ultrasound known as bursts, at frequencies from 0.5 to 18 MHz, have been used to vaporize a variety of sized droplets, requiring peak ultrasound pressures from 0.3 to 8.5 MPa. In general, the vaporisation threshold decreases with increasing droplet diameter and increasing burst length. However, drawing direct comparisons between studies is challenging, because of the tight interplay between droplet composition, concentration, sonication parameters, ambient temperature and pressure, and experimental setup. Figures 4 and 5 compare similar droplet formulations to illustrate the relationship between droplet size, burst length, vaporisation threshold and inertial cavitation threshold.

Figure 4a shows the influence of droplet size on the vaporisation pressure of droplets, as recorded by two independent studies [80, 55], covering a combined diameter range of 2.1 − 22.6 μm Both data sets were formed from DDFP droplets using short burst lengths of 2 or 3 μs, and confirm that increasing droplet diameter decreases the vaporisation threshold. Although the shell material and sonication frequency are different for each study (lipid droplets sonicated at 5.0 MHz [80], albumin droplets sonicated at 3.0 MHz [55]), both data sets follow the trend established by Sheeran *et al.* [80] describing the vaporisation pressure as V(frequency MHz)*(−0.34 ln(droplet diameter μm) + 2.28).

Many studies have shown that increasing burst length lowers the vaporisation threshold [15, 81, 10]. Figure 4b compares studies by Williams *et al.* [15] and Schad *et al.* [10] studying DDFP droplets at three different ambient temperatures over a range of burst lengths 1 μs − 9.6 ms. Calculated based on a cumulative heating effect, Schad *et al.* [10] describe this relationship as (vaporisation pressure$^{\mu}$2 α 1/burst length). Although they acknowledge that

thermal conduction and convection, and mechanical effects from the ultrasound beam have been neglected, the trend shows some similarity to that found by Williams *et al.* [15] at 29°C.

Increasing sonication frequency has been shown to both increase and decrease the vaporisation threshold [9, 55, 10, 15]. The observations ofburst length and frequency offer important insights into the underlying mechanisms behind droplet vaporisation, namely whether this phenomenon is driven by mechanical or thermal processes. In the 2013 study by Williams *et al.* [15] sonication frequencies of 5, 10 and 15 MHz were used to vaporize surfactant-coated 220 nm DDFP droplets using a burst length of 1 ms. The required pressure for vaporisation was found to decrease from 6 MPa to 3.2 MPa with a frequency increase from 5 MHz to 15 MHz. This trend was also observed in the 2010 study by Schad *et al.* [10] when studying the vaporisation thresholds for lipid-coated micron-scale droplets, exposed to 1.7 MHz and 2.9 MHz sonication and 10 ms burst length. The vaporisation threshold was found to decrease by almost half at the higher frequency. This inverse proportionality would suggest a thermal mechanism.

In contrast, Kripfgans *et al.* [55], in the study of albumin-coated micron-scale droplets, found the vaporisation pressure increased with increased frequency, implementing single 3.25 μs bursts at 3 MHz and 4 MHz. This trend would suggest a mechanical mechanism Furthermore, the source of this mechanical nucleation of vaporisation has also been considered, initiating from either outside of the droplet - such as a cavitation bubble impinging on the surface [9] − or from inside the droplet due to acoustic refocusing [12, 11]. Fabiili *et al.* 2009 [59] were trying to access whether inertial cavitation occurring inside the droplet initiated vaporisation. However, the most recent understanding, based on studies exploring superharmonic focusing [11], is that the droplet is converted into a bubble first (through a focused spot of negative pressure generated inside the droplet which spreads through its volume), which is then able to undergo inertial cavitation.

Once a droplet has vaporised into a microbubble it has the potential to undergo inertial cavitation (IC). The pressure required to achieve IC is distinct from the vaporisation threshold and, depending on the therapeutic application, is either strived for (i.e. in sonothrombolysis for the dissolution of clots) or avoided (as in drug delivery to prevent tissue damage). Several studies have measured these two thresholds and the respective influence of sonication frequency, droplet size, ambient temperature and viscosity of the surrounding fluid [59, 17, 10, 81]. At a fixed frequency, the pressure separation between vaporisation and the IC threshold has been found to increase with increasing droplet diameter [59, 10], shown in figure 5. The results also indicate that once the droplet has vaporized, the IC threshold is independent of droplet diameter, remaining between 4 − 6 MPa for albumin or lipid-coated droplets of 1 – 8 μm in size (figure 5). Giesecke *et al.* [9] measured the inertial cavitation threshold of albumin-coated micron-scale droplets and found the pressure threshold increased with increased frequency. They performed sonications at 0.7, 1.1, 2.2 and 3.3 MHz with 100 ms burst length, and identified the inertial cavitation thresholds at 0.6, 1.0, 1.2 and 1.7 MPa respectively.

As the sonication frequency decreases, the separation between thresholds has been found to narrow [10] (figures 5b and 5c), a trend extended to 3.5 MHz by Fabiili *et al.* [59] (figure 5a). In the study of lipid-coated DDFP droplets, Schad *et al.* [10] found that although distinct thresholds could be easily measured at 2.855 MHz and 1.736 MHz, no separation was found between the vaporisation and IC thresholds at 0.578 MHz and IC occurred instantly upon sonication at the lowest pressure used. Fabiili et al. [59] also explored the influence of bulk fluid properties on the vaporisation and IC thresholds, identifying that while gas saturation had little influence, reducing viscosity lowered both thresholds. These findings pose notable implications for therapy and emphasise the importance of tailoring the design and fabrication of droplets for each specific therapeutic application, exploiting droplet vaporisation, IC or both. It is expected that the frequency at which the vaporisation and IC thresholds overlap could be dictated by the droplet size and thus may be controllable.

9. Treatment monitoring

Acoustic monitoring

Utilising droplets for therapy allows for simultaneous treatment and monitoring through a number of different strategies. Most widely exploited are the dynamic acoustic properties of droplets, in particular the change in acoustic impedance upon vaporisation, which allows contrast imaging for B-mode applications [19, 15], illustrated by the increase in acoustic emissions shown in figure 1. Furthermore, the study of harmonic emissions produced by droplets responding to ultrasound has been investigated to monitor bubble size [79]. A decrease in magnitude of the second harmonic in the detected signal was attributed to droplet-to-bubble expansion through resonant size. Sheeran *et al.* [82] have also identified the size-dependent unique acoustic signatures of droplets using lipid-coated perfuorobutane nano-emulsions. Through optical and acoustic measurements, the size and acoustic response of the resulting bubbles were found to follow a damped Minnaert bubble resonance model. By detecting these unique emissions the therapeutic effects of vaporising droplets have the potential to be monitored in real-time.

Magnetic resonance imaging

With the correct PFC core, droplets can also be visualised through MR imaging. As previously mentioned, Rapoport *et al.* [13] illustrates how PFCE droplets can be imaged with 19-F MRI due to the strong emission generated by the 19 fluorine atoms contained within the construct, but with questionable toxicity. An alternative technique for MR imaging is through the incorporation of superparamagnetic nanoparticles [83]. Lee *et al.* [73] created a protocol to embed iron oxide nanoparticles in the shell of protein-polymer droplet for the additional advantage of localised drug delivery through magnetic targeting. Similar constructs were then successfully used for the delivery of siRNA to cancer cells [84].

Magnetic resonance thermometry

When exploiting the thermal effects of vaporized droplets, treatment monitoring may be achieved through magnetic resonance thermometry [85]. Crake *et al.* [86] have shown that changes in proton resonance frequency may be used to measure the temperature change induced by vaporizing DDFP lipid-coated droplets in a polyacrylamide gel phantom.

Furthermore, this technique is paired with passive acoustic mapping (PAM), using an adaptive beamforming algorithm to localise bubble activity through acoustic emissions.

Fluorescence imaging

Droplets can also be fabricated to encapsulate a fluorescence agent, either suspended within the PFC [8] or embedded within the shell [23, 87]. Fluorescence imaging of droplets has been used to assess drug loading and bio-distribution *ex vivo* [35]. Recent advances in nanotechnology and optics have allowed the diverse production of quantum dots [88]. Gorelikov *et al.* [8] have shown the successful encapsulation of quantum dots within PFC droplets for fluorescence imaging *in vitro,* with the additional benefit of lowering the vaporisation threshold.

10. New frontiers

10.1 Drug delivery to the brain

The use of focused ultrasound in the brain is arguably the fastest growing field of biomedical acoustics, and is being applied to enhance the delivery of drugs currently prevented from entering the cerebral tissue by the blood brain barrier [89]. Large molecule drugs are prevented from passing from the blood vessels into the surrounding tissue by tight junctions between endothelial cells. Small molecule drugs that may be able to pass through this barrier are rapidly cleared in the circulation and do not reach the target site in sufficient concentration [90].

Focused ultrasound has been successfully implemented to temporarily increase the permeability of the blood brain barrier, allowing large molecular agents to pass through. Although concerns have been raised around the safety of disrupting the blood brain barrier, and the potential for toxins to pass into the cerebral tissue while the barrier is permeabilised [32], safety studies in many animal models [91] and non-human primates have not shown evidence of this [92, 93, 94]. Further, preliminary clinical investigations have not seen major adverse effects [95, 96, 97]. Generating microbubbles locally for this process may reduce the potential for off-target effects. Successful enhancement of BBB permeability was demonstrated in a murine model using nano-scale droplets [76]. However, the pressure amplitudes required for vaporisation were high (exceeding 0.45 MPa) compared to those required for microbubble - mediated BBB opening. Although no tissue damage was recorded when droplets were used, it is likely that better results can be achieved if lower boiling point droplets are used.

Alternatively, some small lipophilic drugs do not require the blood brain barrier to be breached, but do require encapsulation to prevent premature clearance. Droplets provide an encapsulation method that enables triggered release of small molecule drugs in the brain upon sonication, implemented for neuromodulation for the first time for the suppression of epileptic seizures [35].

10.2 Safety and bio-effects

To enable clinical translation a greater understanding of droplet-induced bio-effects must be developed. Firstly, ensuring the components of the construct are biocompatible is paramount. Liquid-state PFCs have been widely explored in medicine, particularly as a blood substitute due to their ability to carry oxygen. As highlighted by Kripfgans et al. [107], at extremely high concentrations PFCs have been reported to cause pulmonary hyperinflation - over-inflated lungs caused by trapped gas − and respiratory distress in rabbits following intravenous injection at 15 mL/kg [108]. However, typical doses of phase-change droplets contain much lower concentrations of PFCs and show good biocompatibility *in vitro* (0.1 mg/mL after 24 hours of incubation) [96] and *in vivo* (0.3 mL/kg in a rat model) [98].

Secondly, ensuring that vaporisation is responsible only for intended bio-effects is also critical. A recent study ofbio-effects examined haematology and histology in a rat kidney model when exposed to low-boiling point phase-change PFC droplets [98]. Using sonication bursts at 5MHz for 5 cycles, safe vaporisation was achieved at mechanical indices of 0.81 and 1.35. Haemorrhaging in the rat renal tubules was observed at an MI of 1.9. Similarly, in the application of increasing BBB permeability in rats, the use of PFC droplets and associated bio-effects were recorded by Zhang *et al.* [36], where the extravasation of Evans Blue was used to illustrate successful delivery at 1.0 MPa with 1 MHz, but haemorrhage at 1.5 MPa. The mechanism for damage has been attributed to the onset of inertial cavitation [32]. This is a key motivator for many of the threshold studies discussed previously which examine the pressure separation between vaporisation and inertial cavitation. Finding techniques for predicting and monitoring these effects will be critical for safe clinical implementation.

10.3 Clinical translation

Ultimately, for successful translation into the clinic, acoustically active droplets for therapy must be shown to be safe, have higher efficacy than a microbubble contrast agent or free drug, be cost effective, and be formulated and packaged in a way that is easy for storage and medical use. Furthermore, implementing currently approved constructs is often helpful in gaining regulatory approval. Recent creative solutions have included repurposing commercial microbubbles [99], whereby contrast agents are condensed through a cooling and pressuring process to form droplets.

Ultrasound-responsive droplets have found application in a myriad of therapeutic contexts. Developing understanding of droplet vaporisation mechanisms *in vivo,* associated bio-effects and monitoring techniques will enable these responsive nano-scale tools to have a prominent role in the clinic, from ablation to neuromodulation.

Acknowledgements

Funding for this work was provided by The National Institute of Biomedical Imaging and Bioengineering of the National Institutes of Health (R01 EB003268), The Canadian Institutes for Health Research (FRN 119312), and the Canada Research Chair Program (awarded to KH).

References

[1]. Stride EP and Coussios CC, Cavitation and contrast: the use of bubbles in ultrasound imaging and therapy. Proceedings of the Institution of Mechanical Engineers, Part H: Journal of Engineering in Medicine. 2010; 224(2): 171–191.

[2]. Ilyichev VI, Koretz VL and Melnikov NP, Spectral characteristics of acoustic cavitation Ultrasonics. 1989; 27(6): 357–361. [PubMed: 2815406]

[3]. Dayton P, Klibanov A, Brandenburger G and Ferrara K, Acoustic radiation force in vivo: a mechanism to assist targeting of microbubbles, Ultrasound in Medicine and Biology. 1999; 25(8): 1195–1201. [PubMed: 10576262]

[4]. Arvanitis CD, Bazan-Peregrino M, Rifai B, Seymour LW and Coussios CC, Cavitation-enhanced extravasation for drug delivery. Ultrasound in Medicine and Biology. 2011; 37(11): 1838–1852. [PubMed: 21963037]

[5]. Mulvana H, Browning RJ, Luan Y, de Jong N, Tang MX, Eckersley RJ and Stride E, Characterization of contrast agent microbubbles for ultrasound imaging and therapy research, IEEE transactions on ultrasonics, ferroelectrics, and frequency control. 2017; 64(1): 232–251.

[6]. Prigal SJ, Morganbesser LJ and McIntyre FP, Penicillin aerosol in the prevention and treatment of respiratory infections in allergic patients, Journal of Allergy and Clinical Immunology. 1947; 18(5): 325–336.

[7]. Solans C, Izquierdo P, Nolla J, Azemar N and Garcia-Celma MJ, Nano-emulsions. Current opinion in colloid & interface science, 2005; 10(3–4):102–110.

[8]. Gorelikov I, Martin AL, Seo M and Matsuura N, Silica-coated quantum dots for optical evaluation of perfluorocarbon droplet interactions with cells. Langmuir, 2001; 27(24):15024–15033.

[9]. Giesecke T and Hynynen K, Ultrasound-mediated cavitation thresholds of liquid perfluorocarbon droplets in vitro. Ultrasound in Medicine and Biology, 2003; 29(9): 1359–1365. [PubMed: 14553814]

[10]. Schad KC and Hynynen K, In vitro characterization of perfluorocarbon droplets for focused ultrasound therapy. Physics in Medicine & Biology. 2010; 55(17): 4933. [PubMed: 20693614]

[11]. Shpak O, Verweij M, Vos HJ, de Jong N, Lohse D and Versluis M, Acoustic droplet vaporisation is initiated by superharmonic focusing. Proceedings of the National Academy of Sciences. 2014; 111(5): 1697–1702.

[12]. Li DS, Kripfgans OD, Fabiilli ML, Brian Fowlkes J and Bull JL, Initial nucleation site formation due to acoustic droplet vaporisation. Applied physics letters. 2014; 104(6): 063703. [PubMed: 24711671]

[13]. Rapoport N, Nam KH, Gupta R, Gao Z, Mohan P, Payne A, Todd N, Liu X, Kim T, Shea J and Scaife C, Ultrasound-mediated tumor imaging and nanotherapy using drug loaded, block copolymer stabilized perfluorocarbon nanoemulsions. Journal of Controlled Release, 2011; 153(1): 4–15. [PubMed: 21277919]

[14]. Amir N, Green D, Kent J, Xiang Y, Gorelikov I, Seo M, Blacker M, Janzen N, Czorny S, Valliant JF and Matsuura N, 18F-Labeled perfluorocarbon droplets for positron emission tomography imaging. Nuclear medicine and biology, 2017; 54: 27–33. [PubMed: 28863330]

[15]. Williams R, Wright C, Cherin E, Reznik N, Lee M, Gorelikov I, Foster FS, Matsuura N and Burns PN, Characterization of submicron phase-change perfluorocarbon droplets for extravascular ultrasound imaging of cancer. Ultrasound in Medicine and Biology, 2013; 39(3): 475–489. [PubMed: 23312960]

[16]. Sheeran PS, Matsuura N, Borden MA, Williams R, Matsunaga TO, Burns PN and Dayton PA, Methods of generating submicrometer phase-shift perfluorocarbon droplets for applications in medical ultrasonography. IEEE transactions on ultrasonics, ferroelectrics, and frequency control, 2017b; 64(1): 252–263.

[17]. Zhang P and Porter T, An in vitro study of a phase-shift nanoemulsion: a potential nucleation agent for bubble-enhanced HIFU tumor ablation. Ultrasound in Medicine and Biology, 2010; 36(11): 1856–1866. [PubMed: 20888685]

[18]. Pajek D, Burgess A, Huang Y and Hynynen K, High-intensity focused ultrasound sonothrombolysis: the use of perfluorocarbon droplets to achieve clot lysis at reduced acoustic power. Ultrasound in Medicine and Biology, 2014; 40(9): 2151–2161. [PubMed: 25023095]

[19]. Kripfgans OD, Fowlkes JB, Miller DL, Eldevik OP and Carson PL, Acoustic droplet vaporisation for therapeutic and diagnostic applications. Ultrasound in Medicine and Biology, 2000; 26(7): 1177–1189. [PubMed: 11053753]

[20]. Radhakrishnan K, Holland CK and Haworth KJ, Scavenging dissolved oxygen via acoustic droplet vaporisation. Ultrasonics sonochemistry, 2016; 31: 394–403. [PubMed: 26964964]

[21]. Haworth KJ, Arunkumar P, Goldstein BH, Su H, Mercado-Shekhar KP, Privitera EM, Srivastava R, Holland CK and Redington AN, Dissolved oxygen scavenging by acoustic droplet vaporisation using intravascular ultrasound In Ultrasonics Symposium (IUS), 2017; IEEE International 1–4.

[22]. Fix SM, Novell A, Yun Y, Dayton PA and Arena CB, An evaluation of the sonoporation potential of low-boiling point phase-change ultrasound contrast agents in vitro. Journal of Therapeutic Ultrasound, 2017; 5(1): 7. [PubMed: 28127427]

[23]. Gao Z, Kennedy AM, Christensen DA and Rapoport NY, Drug-loaded nano/microbubbles for combining ultrasonography and targeted chemotherapy. Ultrasonics, 2008; 48(4): 260–270. [PubMed: 18096196]

[24]. Rapoport N, Payne A, Dillon C, Shea J, Scaife C and Gupta R, Focused ultrasound-mediated drug delivery to pancreatic cancer in a mouse model. Journal of therapeutic ultrasound, 2013; 1(1): 11. [PubMed: 25516800]

[25]. Baronzio G, Fiorentini G and Cogle CR, Cancer microenvironment and therapeutic implications. Berlin, Germany: Springer; 2009.

[26]. Rapoport N, Phase-shift, stimuli-responsive perfluorocarbon nanodroplets for drug delivery to cancer. Wiley Interdisciplinary Reviews: Nanomedicine and Nanobiotechnology, 2012; 4(5): 492–510. [PubMed: 22730185]

[27]. Cao Y, Chen Y, Yu T, Guo Y, Liu F, Yao Y, et al., Drug Release from Phase-Changeable Nanodroplets Triggered by Low-Intensity Focused Ultrasound. Theranostics. 2018; 8(5): 1327. [PubMed: 29507623]

[28]. Gao D, Gao J, Xu M, Cao Z, Zhou L, Li Y, et al., Targeted ultrasound-triggered phase transition nanodroplets for her2-overexpressing breast cancer diagnosis and gene transfection. Molecular pharmaceutics, 2017; 14(4): 984–998. [PubMed: 28282145]

[29]. Hingot V, Bezagu M, Errico C, Desailly Y, Bocheux R, et al., Subwavelength far-field ultrasound drug-delivery. Applied Physics Letters, 2016; 109(19): 194102.

[30]. Rojas JD, Borden MA and Dayton PA, Effect of boundary constraints and hydrostatic pressure on the vaporisation threshold of low boiling-point phase-change contrast agents In Ultrasonics Symposium (IUS), 2017; IEEE International 1–4.

[31]. Lin S, Zhang G, Leow CH and Tang MX, Effects of microchannel confinement on acoustic vaporisation of ultrasound phase change contrast agents. Physics in Medicine & Biology, 2017; 62(17): 6884. [PubMed: 28718774]

[32]. Wu SY, Fix SM, Arena CB, Chen CC, Zheng W, Olumolade OO, Papadopoulou V, Novell A, Dayton PA and Konofagou EE, Focused ultrasound-facilitated brain drug delivery using optimized nanodroplets: vaporisation efficiency dictates large molecular delivery. Physics in Medicine & Biology, 2018; 63(3): 035002. [PubMed: 29260735]

[33]. Lipsman N, Schwartz ML, Huang Y, Lee L, Sankar T, Chapman M, Hynynen K and Lozano AM, MR-guided focusec ultrasound thalamotomy for essential tremor: a proof-of-concept study. The Lancet Neurology, 2013; 12(5): 462–468. [PubMed: 23523144]

[34]. Hynynen K, McDannold N, Vykhodtseva N and Jolesz FA, Noninvasive MR imaging-guided focal opening of the blood-brain barrier in rabbits. Radiology, 2001; 220(3): 640–646. [PubMed: 11526261]

[35]. Airan R, Neuromodulation with nanoparticles. Science, 2017; 357(6350): 465–465. [PubMed: 28774921]

[36]. Zhang X, Hu J, Zhao G, Huang N, Tan Y, Pi L, Huang Q, Wang F, Wang Z, Wang Z and Cheng Y, PEGylated PLGA-based phase shift nanodroplets combined with focused ultrasound for blood brain barrier opening in rats. Onco target, 2017; 8(24): 38927.

[37]. McDannold N, Vykhodtseva N and Hynynen K, Targeted disruption of the blood-brain barrier with focused ultrasound: association with cavitation activity. Physics in Medicine & Biology, 2006; 51(4): 793. [PubMed: 16467579]

[38]. Fry WJ, Mosberg WH Jr, Barnard JW and Fry FJ, Production of focal destructive lesions in the central nervous system with ultrasound. Journal of neurosurgery, 1954; 11(5): 471–478. [PubMed: 13201985]

[39]. Fry FJ, Ades HW and Fry WJ, Production of reversible changes in the central nervous system by ultrasound. Science, 1958; 127(3289): 83–84. [PubMed: 13495483]

[40]. Legon W, Sato TF, Opitz A, Mueller J, Barbour A, Williams A and Tyler WJ, Transcranial focused ultrasound modulates the activity of primary somatosensory cortex in humans. Nature neuroscience, 2014; 17(2): 322. [PubMed: 24413698]

[41]. Scarcelli T, Jordao JF, O'reilly MA, Ellens N, Hynynen K and Aubert I, Stimulation of hippocampal neurogenesis by transcranial focused ultrasound and microbubbles in adult mice. Brain Stimulation: Basic, Translational, and Clinical Research in Neuromodulation, 2014; 7(2): 304–307.

[42]. Lyon PC, Griffiths LF, Lee J, Chung D, Carlisle R, Wu F, Middleton MR, Gleeson FV and Coussios CC, Clinical trial protocol for TARDOX: a phase I study to investigate the feasibility of targeted release of lyso-thermosensitive liposomal doxorubicin (ThermoDox®) using focused ultrasound in patients with liver tumours. Journal of therapeutic ultrasound, 2017; 5(1): 28. [PubMed: 29118984]

[43]. Dimcevski G, Kotopoulis S, Bjånes T, Hoem D, Schjøtt J, Gjertsen BT, Biermann M, Molven A, Sorbye H, McCormack E and Postema M, A human clinical trial using ultrasound and microbubbles to enhance gemcitabine treatment of inoperable pancreatic cancer. Journal of Controlled Release, 2016; 243: 172–181. [PubMed: 27744037]

[44]. Ter Haar G, Therapeutic applications of ultrasound. Progress in biophysics and molecular biology, 2007; 93(1–3): 111–129. [PubMed: 16930682]

[45]. Coussios CC and Roy RA, Applications of acoustics and cavitation to noninvasive therapy and drug delivery. Annu. Rev. Fluid Mech, 2008; 40: 395–420.

[46]. Lea-Banks H, Teo B, Stride E and Coussios CC, The effect of particle density on ultrasound-mediated transport of nanoparticles. Physics in Medicine & Biology, 2016; 61(22): 7906. [PubMed: 27779121]

[47]. Lentacker I, De Cock I, Deckers R, De Smedt SC and Moonen CTW, Understanding ultrasound induced sonoporation: definitions and underlying mechanisms. Advanced drug delivery reviews, 2014; 72: 49–64. [PubMed: 24270006]

[48]. Unger EC, McCreery TP, Sweitzer RH, Caldwell VE and Wu Y, Acoustically active lipospheres containing paclitaxel: a new therapeutic ultrasound contrast agent. Investigative radiology, 1998; 33(12): 886–892. [PubMed: 9851823]

[49]. Unger EC, Hersh E, Vannan M, Matsunaga TO and McCreery T, Local drug and gene delivery through microbubbles. Progress in cardiovascular diseases, 2001; 44(1): 45–54. [PubMed: 11533926]

[50]. O'Reilly MA and Hynynen K, Blood-brain barrier: real-time feedback-controlled focused ultrasound disruption by using an acoustic emissions-based controller. Radiology, 2012; 263(1): 96–106. [PubMed: 22332065]

[51]. Sun T, Zhang Y, Power C, Alexander PM, Sutton JT, Aryal M, Vykhodtseva N, Miller EL and McDannold NJ, Closed-loop control of targeted ultrasound drug delivery across the blood-brain/tumor barriers in a rat glioma model. Proceedings of the National Academy of Sciences, 2017; 114(48): E10281–E10290.

[52]. O'Reilly MA, Jones RM and Hynynen K, Three-dimensional transcranial ultrasound imaging of microbubble clouds using a sparse hemispherical array. IEEE Transactions on Biomedical Engineering, 2014; 61(4): 1285–1294. [PubMed: 24658252]

[53]. Zhang M, Fabiilli ML, Haworth KJ, Fowlkes JB, Kripfgans OD, Roberts WW, Ives KA and Carson PL, Initial investigation of acoustic droplet vaporisation for occlusion in canine kidney. Ultrasound in Medicine and Biology, 2010; 36(10): 1691–1703. [PubMed: 20800939]

[54]. Apfel RE, Activatable infusable dispersions containing drops of a superheated liquid for methods of therapy and diagnosis Patent 5,840,276, Apfel Enterprises. Inc., 1998.

[55]. Kripfgans OD, Fabiilli ML, Carson PL and Fowlkes JB, On the acoustic vaporisation of micrometer-sized droplets. The Journal of the Acoustical Society of America, 2004; 116(1): 272–281. [PubMed: 15295987]

[56]. Seo M, Gorelikov I, Williams R and Matsuura N, Microfuidic assembly of monodisperse, nanoparticle-incorporated perfuorocarbon microbubbles for medical imaging and therapy. Langmuir, 2010; 26(17): 13855–13860. [PubMed: 20666507]

[57]. Christopher GF and Anna SL, Microfuidic methods for generating continuous droplet streams. Journal of Physics D: Applied Physics, 2007; 40(19): R319.

[58]. Rapoport N, Drug-loaded perfuorocarbon nanodroplets for ultrasound-mediated drug delivery In Therapeutic Ultrasound (pp. 221–241). Springer, Cham; 2016.

[59]. Fabiilli ML, Haworth KJ, Fakhri NH, Kripfgans OD, Carson PL and Fowlkes JB, The role of inertial cavitation in acoustic droplet vaporisation. IKKK transactions on ultrasonics, ferroelectrics, and frequency control, 2009; 56(5).

[60]. Marmottant P, van der Meer S, Emmer M, Versluis M, de Jong N, Hilgenfeldt S and Lohse D, A model for large amplitude oscillations of coated bubbles accounting for buckling and rupture. The Journal of the Acoustical Society of America, 2005; 118(6): 3499–3505.

[61]. Luan Y, Lajoinie G, Gelderblom E, Skachkov I, van der Steen AF, Vos HJ, Versluis M and De Jong N, Lipid shedding from single oscillating microbubbles. Ultrasound in medicine and biology, 2014; 40(8): 1834–1846. [PubMed: 24798388]

[62]. Lentacker I, Geers B, Demeester J, De Smedt SC and Sanders NN, Design and evaluation of doxorubicin-containing microbubbles for ultrasound-triggered doxorubicin delivery: cytotoxicity and mechanisms involved. Molecular Therapy, 2010; 18(1): 101–108. [PubMed: 19623162]

[63]. Kawabata KI, Sugita N, Yoshikawa H, Azuma T and Umemura SI, Nanoparticles with multiple perfuorocarbons for controllable ultrasonically induced phase shifting. Japanese journal of applied physics, 2005; 44(6S): 4548.

[64]. Lanza GM, Wallace KD, Scott MJ, Cacheris WP, Abendschein DR, Christy DH, Sharkey AM, Miller JG, Gaffney PJ and Wickline SA, A novel site-targeted ultrasonic contrast agent with broad biomedical application. Circulation, 1996; 94(12): 3334–3340. [PubMed: 8989148]

[65]. Schottler S, Becker G, Winzen S, Steinbach T, Mohr K, Landfester K, Mailander V and Wurm FR, Protein adsorption is required for stealth effect of poly (ethylene glycol)-and poly (phosphoester)-coated nanocarriers. Nature nanotechnology, 2016; 11(4): 372.

[66]. Rapoport N, Physical stimuli-responsive polymeric micelles for anti-cancer drug delivery. Progress in Polymer Science, 2007; 32(8–9): 962–990.

[68]. Lacour T, Guedra M, Valier-Brasier T and Coulouvrat F, A model for acoustic vaporisation dynamics of a bubble/droplet system encapsulated within a hyperelastic shell. The Journal of the Acoustical Society of America, 2018; 143(1): 23–37. [PubMed: 29390781]

[69]. Mountford PA, Thomas AN and Borden MA, Thermal activation of superheated lipid-coated perfluorocarbon drops. Langmuir, 2015; 31(16): 4627–4634. [PubMed: 25853278]

[70]. Tirotta I, Mastropietro A, Cordiglieri C, Gazzera L, Baggi F, Baselli G, Bruzzone MG, Zucca I, Cavallo G, Terraneo G and Baldelli Bombelli F, A superfluorinated molecular probe for highly sensitive in vivo 19F-MRI. Journal of the American Chemical Society, 2014; 136(24): 8524–8527. [PubMed: 24884816]

[71]. Jacoby C, Temme S, Mayenfels F, Benoit N, Krafft MP, Schubert R, Schrader J and Flögel U, Probing different perfluorocarbons for in vivo inflammation imaging by 19F MRI: image reconstruction, biological half - lives and sensitivity. NMR in Biomedicine, 2014; 27(3): 261–271. [PubMed: 24353148]

[72]. Martin AL, Seo M, Williams R, Belayneh G, Foster FS and Matsuura N, Intracellular growth of nanoscale perfluorocarbon droplets for enhanced ultrasound-induced phase-change conversion. Ultrasound in Medicine and Biology, 2012; 38(10): 1799–1810. [PubMed: 22920544]

[73]. Lee JY, Carugo D, Crake C, Owen J, de Saint Victor M, Seth A, Coussios C and Stride E, Nanoparticle-Loaded Protein-Polymer Nanodroplets for Improved Stability and Conversion Efficiency in Ultrasound Imaging and Drug Delivery. Advanced Materials, 2015; 27(37): 5484–5492. [PubMed: 26265592]

[74]. Matsunaga TO, Sheeran PS, Luois S, Streeter JE, Mullin LB, Banerjee B and Dayton PA, Phase-change nanoparticles using highly volatile perfluorocarbons: toward a platform for extravascular ultrasound imaging. Theranostics, 2013; 2(12): 1185.

[75]. Wang CH, Kang ST and Yeh CK, Superparamagnetic iron oxide and drug complex-embedded acoustic droplets for ultrasound targeted theranosis. Biomaterials, 2013; 34(7): 1852–1861. [PubMed: 23219326]

[76]. Chen CC, Sheeran PS, Wu SY, Olumolade OO, Dayton PA and Konofagou EE, Targeted drug delivery with focused ultrasound-induced blood-brain barrier opening using acoustically-activated nanodroplets. Journal of Controlled Release, 2013; 172(3): 795–804. [PubMed: 24096019]

[77]. Miles CJ, Doering CR and Kripfgans OD, Nucleation pressure threshold in acoustic droplet vaporisation. Journal of Applied Physics, 2016; 120(3): 034903.

[78]. European Medicines Agency, 2001, Annex I: SonoVue - Summary of Product Characteristics, http://www.ema.europa.eu/docs/en_GB/document_library/EPAR_-_Product_Information/human/000303/WC500055380.pdf

[79]. Reznik N, Williams R and Burns PN, Investigation of vaporized submicron perfluorocarbon droplets as an ultrasound contrast agent. Ultrasound in Medicine and Biology, 2011; 37(8): 1271–1279. [PubMed: 21723449]

[80]. Sheeran PS, Luois S, Dayton PA and Matsunaga TO, Formulation and acoustic studies of a new phase-shift agent for diagnostic and therapeutic ultrasound. Langmuir, 2011; 27(17): 10412–10420. [PubMed: 21744860]

[81]. Kripfgans OD, Zhang M, Fabiilli ML, Carson PL, Padilla F, Swanson SD, Mougenot C, Brian Fowlkes J and Mougenot C, Acceleration of ultrasound thermal therapy by patterned acoustic droplet vaporisation. The Journal of the Acoustical Society of America, 2014; 135(1): 537–544. [PubMed: 24437794]

[82]. Sheeran PS, Matsunaga TO and Dayton PA, Phase change events of volatile liquid perfluorocarbon contrast agents produce unique acoustic signatures. Physics in Medicine & Biology, 2013; 59(2): 379. [PubMed: 24351961]

[83]. Crake C, Owen J, Smart S, Coviello C, Coussios CC, Carlisle R and Stride E, Enhancement and passive acoustic mapping of cavitation from fuorescently tagged magnetic resonance-visible magnetic microbubbles in vivo. Ultrasound in Medicine and Biology, 2016; 42(12): 3022–3036. [PubMed: 27666788]

[84]. Lee JY, Crake C, Teo B, Carugo D, de Saint Victor M, Seth A and Stride E, Ultrasound - Enhanced siRNA Delivery Using Magnetic Nanoparticle-Loaded Chitosan-Deoxycholic Acid Nanodroplets. Advanced Healthcare Materials, 2017; 6(8).

[85]. Ishihara Y, Calderon A, Watanabe H, Okamoto K, Suzuki Y, Kuroda K and Suzuki Y, A precise and fast temperature mapping using water proton chemical shift. Magnetic resonance in medicine, 1995; 34(6): 814–823. [PubMed: 8598808]

[86]. Crake C, Meral FC, Burgess MT, Papademetriou IT, McDannold NJ and Porter TM, Combined passive acoustic mapping and magnetic resonance thermometry for monitoring phase-shift nanoemulsion enhanced focused ultrasound therapy. Physics in Medicine & Biology, 2017; 62(15): 6144. [PubMed: 28590938]

[87]. Mountford PA, Sirsi SR and Borden MA, Condensation phase diagrams for lipid-coated perfuorobutane microbubbles. Langmuir, 2014; 30(21): 6209–6218. [PubMed: 24824162]

[88]. SalmanOgli A, Nanobio applications of quantum dots in cancer: imaging, sensing, and targeting. Cancer nanotechnology, 2011; 2(1–6): 1–19. [PubMed: 26069481]

[89]. Hynynen K, Ultrasound for drug and gene delivery to the brain. Advanced drug delivery reviews, 2008; 60(10): 1209–1217. [PubMed: 18486271]

[90]. Saraiva C, Praga C, Ferreira R, Santos T, Ferreira L and Bernardino L, Nanoparticle-mediated brain drug delivery: overcoming blood-brain barrier to treat neurodegenerative diseases. Journal of Controlled Release, 2016; 235: 34–47. [PubMed: 27208862]

[91]. O'Reilly MA and Hynynen K, Ultrasound enhanced drug delivery to the brain and central nervous system. International Journal of Hyperthermia, 2012; 8(4): 386–396.

[92]. McDannold N, Arvanitis CD, Vykhodtseva N and Livingstone MS, Temporary disruption of the blood-brain barrier by use of ultrasound and microbubbles: safety and efficacy evaluation in rhesus macaques. Cancer research, 2012; 72(14): 3652–3663. [PubMed: 22552291]

[93]. Marquet F, Tung YS, Teichert T, Ferrera VP and Konofagou EE, Noninvasive, transient and selective blood-brain barrier opening in non-human primates in vivo. PloS one, 2011; 6(7): e22598. [PubMed: 21799913]

[94]. Downs ME, Buch A, Sierra C, Karakatsani ME, Chen S, Konofagou EE and Ferrera VP, Long-term safety of repeated blood-brain barrier opening via focused ultrasound with microbubbles in non-human primates performing a cognitive task. PloS one, 2015; 10(5): e0125911. [PubMed: 25945493]

[95]. Carpentier A, Canney M, Vignot A, Reina V, Beccaria K, Horodyckid C, Karachi C, Leclercq D, Lafon C, Chapelon JY and Capelle L, Clinical trial of blood-brain barrier disruption by pulsed ultrasound. Science translational medicine, 2016; 8(343): 343.

[96]. Huang Y, Alkins R, Chapman M, Perry J, Sahgal A and Trudeau M, Initial experience in a pilot study of blood-brain barrier opening for chemo-drug delivery to brain tumors by MR-guided focused ultrasound. In 24th Annual Meeting of the International Society for Magnetic Resonance in Medicine, 2016.

[97]. Lipsman N, Meng Y, Bethune AJ, Huang Y, Lam B, Masellis M, Herrmann N, Heyn C, Aubert I, Boutet A and Smith GS, Blood-brain barrier opening in Alzheimer's disease using MR-guided focused ultrasound. Nature communications, 2018; 9(1): 2336.

[98]. Nyankima AG, Rojas JD, Cianciolo R, Johnson KA and Dayton PA, In vivo Assessment of the Potential for Renal Bio-Effects from the Vaporisation of Perfuorocarbon Phase-Change Contrast Agents. Ultrasound in medicine & biology, 2018; 44(2): 368–376. [PubMed: 29254872]

[99]. Sheeran PS, Yoo K, Williams R, Yin M, Foster FS and Burns PN, More than bubbles: creating phase-shift droplets from commercially available ultrasound contrast agents. Ultrasound in Medicine and Biology, 2017; 43(2): 531–540. [PubMed: 27727022]

[100]. Nino MRR and Patino JR, Surface tension of bovine serum albumin and tween 20 at the air-aqueous interface. Journal of the American Oil Chemists' Society, 1998; 75(10): 1241.

[101]. Kovalchuk NM, Trybala A, Starov V, Matar O and Ivanova N, Fluoro-vs hydrocarbon surfactants: Why do they differ in wetting performance?. Advances in colloid and interface science, 2014; 210: 65–71. [PubMed: 24814169]

[102]. Joos P and Demel RA, The interaction energies of cholesterol and lecithin in spread mixed monolayers at the air-water interface. Biochimica et Biophysica Acta (BBA)-Biomembranes, 1969; 183(3): 447–457. [PubMed: 5822817]

[103]. Feller SE, Venable RM and Pastor RW, Computer simulation of a DPPC phospholipid bilayer: structural changes as a function of molecular surface area. Langmuir, 1997; 13(24): 6555–6561.

[104]. Amooey AA and Fazlollahnejad M, Study of Surface Tension of Binary Mixtures of Poly (Ethylene Glycol) in Water and Poly (Propylene Glycol) in Ethanol and Its Modeling Using Neural Network. Iranian Journal of Chemical Engineering, 2014; 11(1): 19–29.

[105]. Prasad KN, Luong TT, Paris ATF, Vaution C, Seiller M and Puisieux F, Surface activity and association of ABA polyoxyethylene—polyoxypropylene block copolymers in aqueous solution. Journal of Colloid and Interface science, 1979; 69(2): 225–232.

[106]. Sheeran PS, Luois SH, Mullin LB, Matsunaga TO and Dayton PA, Design of ultrasonically-activatable nanoparticles using low boiling point perfluorocarbons. Biomaterials, 2012; 33(11): 3262–3269. [PubMed: 22289265]

[107]. Kripfgans OD, Orifici CM, Carson PL, Ives KA, Eldevik OP and Fowlkes JB, 2005 Acoustic droplet vaporization for temporal and spatial control of tissue occlusion: a kidney study. IEEE transactions on ultrasonics, ferroelectrics, and frequency control, 52(7), pp.1101–1110.

[108]. Eckmann DM, Swartz MA, Glucksberg MR, Gavriely N and Grotberg JB, 1998 Perfluorocarbon induced alterations in pulmonary mechanics. Artificial Cells, Blood Substitutes, and Biotechnology, 26(3), pp.259–271.

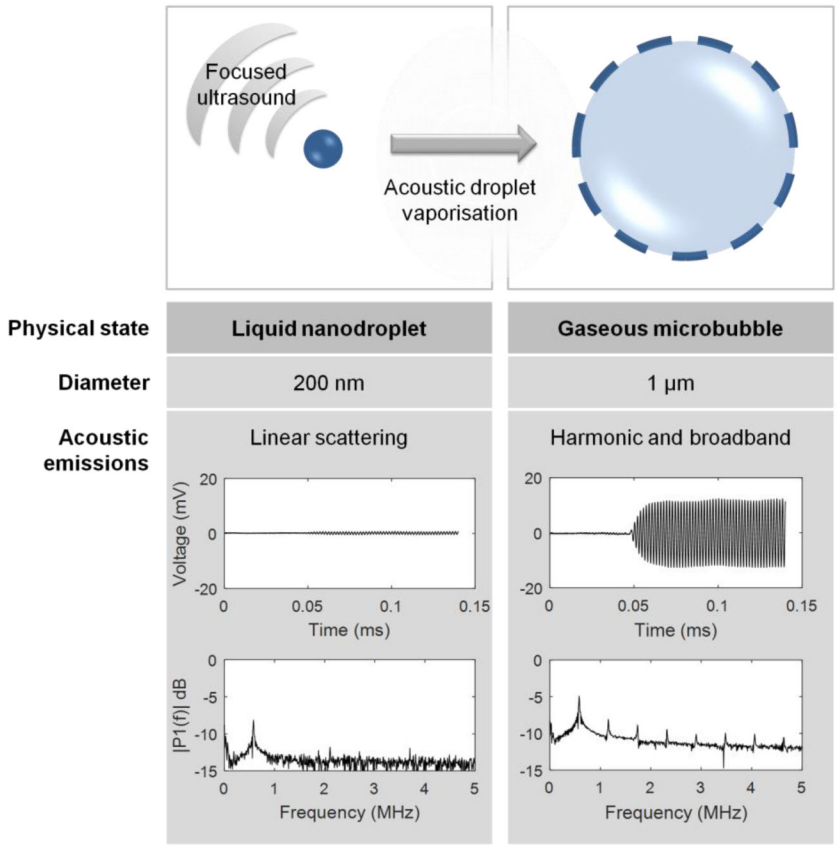

Figure 1.

Schematic of acoustic droplet vaporisation with example 200 nm liquid droplet vaporising into a 1 µm gaseous microbubble when sonicated with focused ultrasound. Unique acoustic emissions are produced in each state, illustrated with example voltagetraces and frequency spectra detected with an ultrasound receiver.

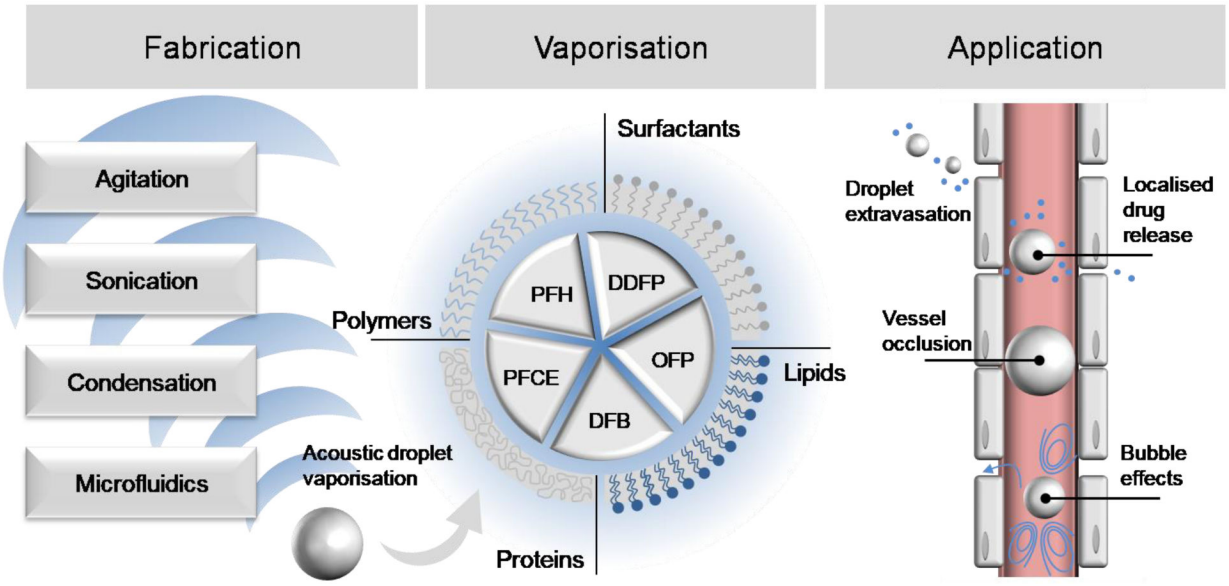

Figure 2.

Schematic of the fabrication techniques, shell and core compositions - including perfluorohexane (PFH), dodecafluoropentane (DDFP), octafluoropropane (OFP) decafluorobutane (DFB) and perfluoro −15-crown-5-ether (PFCE) – and potential applications of droplets for therapy. By defining the design criteria, bespoke droplets may be fabricated with tech niques and materials most appropriate for the intended application.

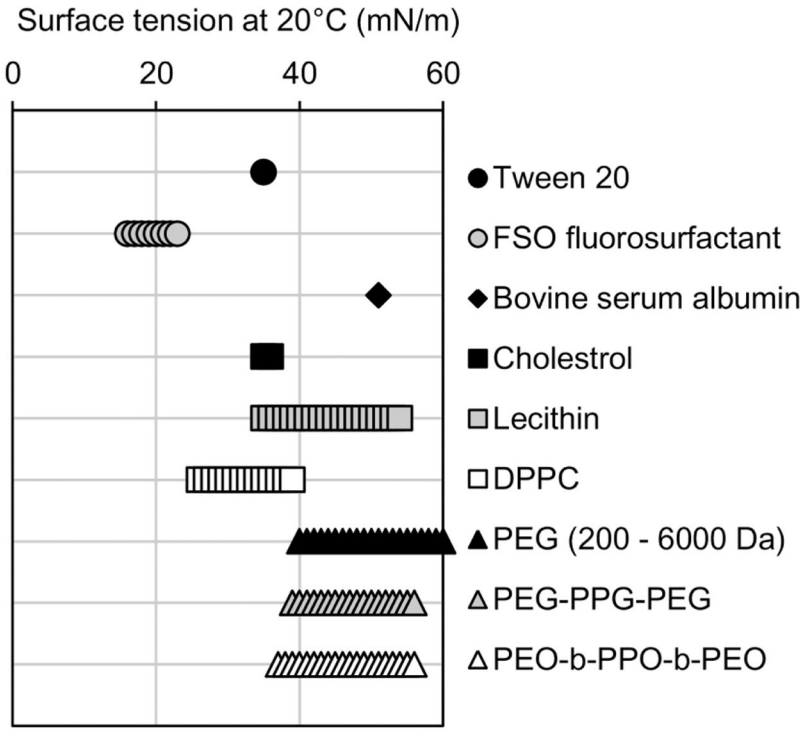

Figure 3.
Summary of surface tension values at 20°C of various surfactants (●), albumin (◆), lipids (■) and polymers (▲).

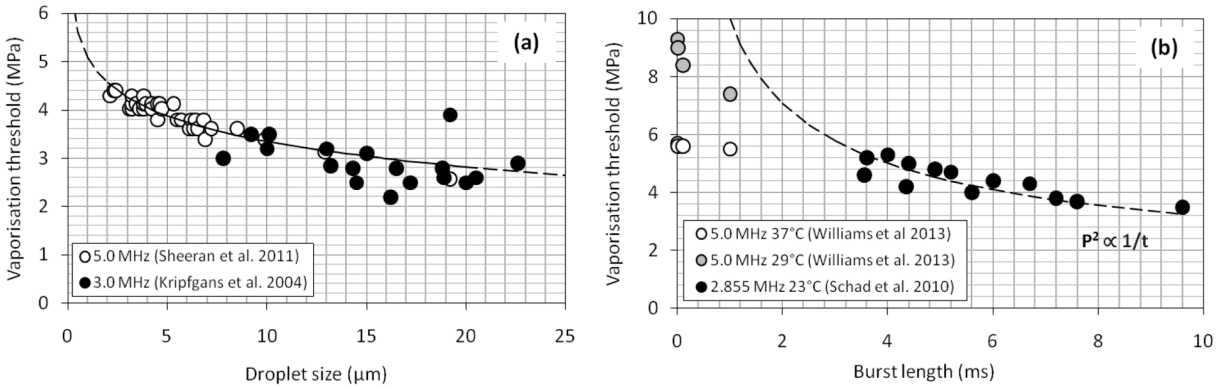

Figure 4.

Vaporisation threshold of PFC droplets is reduced by increasing **(a)** droplet size and **(b)** burst length, as illustrated through studies by Sheeran et al. [80], Kripfgans et al.[55], Williams et al. [15] and Schad et al. [10].

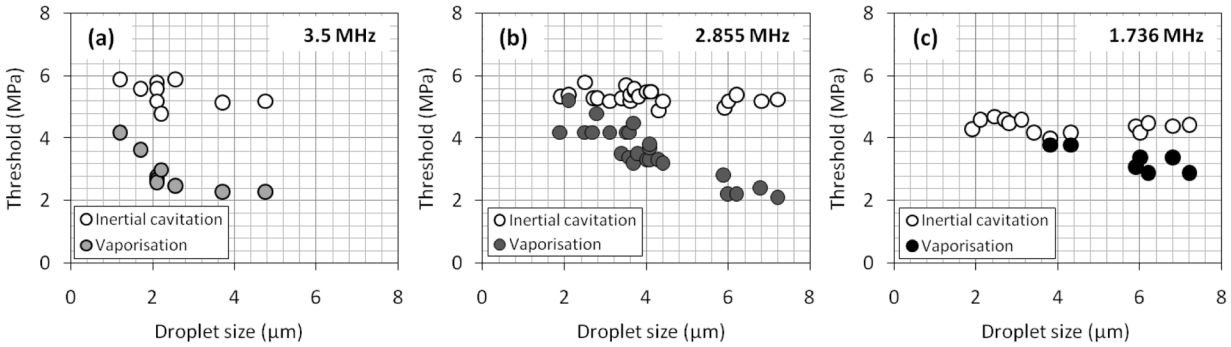

Figure 5.

Vaporisation and inertial cavitation thresholds of PFC droplets at **(a)** 3.5 MHz (Fabiilli et al [59]), **(b)** 2.855 MHz (Schad et al. [10]) and **(c)** 1.736 MHz (Schad et al. [10]), where the separation between thresholds decreases with decreasing frequency.

Table 1.

Summary of common droplet fabrication techniques and associated references.

Technique	Category	Achieved droplet size range	Size distribution	Reproducibility	Ease and speed of fabrication in bulk	References
Hand-shaken	*Agitation*	10 – 100 μm	Wide	Low	High	Apfel [54] Kripfgans *et al.* [55]
Amalgamator	*Agitation*	1 – 5 μm	Wide	Low	High	Kripfgans *et al.* [81] Fabiilli *et al.* [59]
Glass beads and mini beadbeater	*Agitation*	1 – 2 μm	Wide	Low	High	Giesecke *et al.* [9]
Sonicationbath	*Sonication*	0.1 – 2 μm	Moderate	Moderate	High	Gao *et al.* [23]
Tip sonicator	*Sonication*	100 – 800 μm	Moderate	Moderate	High	Williams *et al.* [15] Rapoport *et al.* [24] Pajek *et al.* [18] Airan *et al.* [35]
Condensation of microbubbles	*Condensation*	0.5 – 2 μm	Dependent on precursor microbubbles		Moderate	Sheeran *et al.* [80]
Condensation of commercial contrast agents	*Condensation*	200 – 400 μm	Dependent on precursor microbubbles		Moderate	Sheeran *et al.* [99]
Commercial micro tlnidizcr	*Microfluidic*	1 – 10 μm	Narrow	Moderate	Low	Schad *et al.* [10]
Bespoke microfluidc device	*Microfluidic*	0.5 – 50 μm	Narrow	High	Low	Seo *et al.* [56] Christopher *et al.* [57]

Table 2.

Summary of shell materials grouped by coating type and surface tension values measured at 20°C from cited references.

Compound name	Coating type	Surface tension at 20°C (mN/m)	Reference
Tween 20	Surfactant	35	Niño *et al.* [100]
Zonyl FSO fluorosurfactant		16 – 23	Kovalchuk *et al.* [101]
Bovine serum albumin (BSA)	Albumin	51	Niño *et al.* [100]
Cholestrol	Lipid	35 – 36	Joos *et al.* [102]
Lecithin		35 – 54	Joos *et al.* [102]
Dipalmitoyl-phosphatidylcholine (DPPC)		26 – 39	Feller *et al.* [103]
PEG (200–6000 Da)	Polymer	40 – 60	Amooey *et al.* [104]
PEG-PPG-PEG		39 – 56	Prasad *et al.*. [105]
PEO-b-PPO-b-PEO		37 – 56	Prasad *et al.* [105]

Table 3.

Summary of commonly used perfluorocarbons, acronyms, chemical properties and associated references.

Compound name Synonym	Acronym	Molecular formula	Molecular weight*(g/mol)	Density at 20°C*(g/mL)	Boiling point*(°C)	Droplet reference
Octafluoropropane *Perfluoropropane*	(OFP)	(C_3F_8)	188.02	1.35	−39	Fix *et al.* [22] Nyankima *et al.* [98] Sheeran *et al.* [106, 99] Wu *et al.* [32]
Decafluorobutane *Perfluorobutane*	(DFB)	(C_4F_{10})	238.03	1.52	−2	Sheeran *et al.* [106, 16] Wu *et al.* [32]
Dodecafluorope ntane *Perfluoropentane*	(DDFP)	(C_5F_{12})	288.03	1.66	29	Kripfgans *et al.* [55, 81] P. Zhang *et al.* [17] Giesecke *et al.* [9] Fabiilli *et al.* [59] Schad *et al.* [10] Williams *et al.* [15] Pajek *et al.* [18] Airan *et al.* [35] Radhakrishnan *et al.* [20] Zhang *et al.* [36]
Decafluoropentane *2H,3H-Perfluoropentane*	(DFP)	(C_5F_{10})	252.05	1.60	55	Kawabata *et al.* [63]
Perfluorohexane *Perfluoro-n-hexane*	(PFH)	(C_6F_{14})	338.04	1.67	58	Giesecke *et al.* [9] Fabiilli *et al.* [59]
Perfluoromethylcyclo-hexane *Tetradecaflu oromethyl-cyclohexane*	(PFM)	(C_7F_{14})	350.05	1.79	76	Giesecke *et al.* [9]
Perfluorooctane *Octadecafluorooctane*	(PFO)	(C_8F_{18})	438.06	1.76	103	Fabiilli *et al.* [59]
Perfluoro-15-crown-5-ether	(PFCE)	($C_{10}F_{20}O_5$)	580.07	1.30	146	Rapoport *et al.* [13]
Perfluorodichlorooctane	(PFD)	($C_8C_{12}F_{16}$)	470.96	1.70	176	Lanza *et al.* [64]

*Values taken from Sigma Aldrich and Synquest Laboratories

Table 4.

Summary of approximate droplet diameters required for various therapeutic applications.

Application	Approximate droplet diameter	Reference
Vessel occlusion	> 3 μm	M. Zhang *et al.* [53]
Systemic circulation	< 1 μm	M. Zhang *et al.* [53]
Extra vasal ion in tumour tissue	< 500 nm	Rapoport *et al.* [26]
Extravasation in healthy tissue	< 20 nm	Baronzio *et al.* [25]